AN ABSTRACT OF THE THESIS OF

Yang Zhang for the degree of Master of Science in Electrical and Computer Engineering presented on May 10, 2017.

Title: Coverage Algorithms for WiFO: A Hybrid WiFi-FSO Femtocell Communication System.

Abstract approved:

_____

Thinh Nguyen

Coverage algorithms for deployment of WiFO - a hybrid femtocell architecture based on WiFi and Free Space Optical (FSO) technologies are studied to significantly increase wireless throughput of existing WiFi networks. In contrast with existing WiFi networks, WiFO incorporates small cell size, line of sight transmissions, and the Gaussian attenuation model of light intensity into the design of the coverage algorithms. Specifically, two types of coverage scenarios - the non-overlapped and the overlapped coverage are presented. For the non-overlapped coverage, we show the bounds of coverage efficiency for a finite rectangle area based on a simple model. For the overlapped coverage, user's SNR profiles are assumed to be given. Using these, three algorithms for determining the optimized deployment based user's SNR profiles and Gaussian light attenuation models are proposed and evaluated. Simulation results are provided to verify the proposed algorithms.

Coverage Algorithms for WiFO: A Hybrid WiFi-FSO Femtocell Communication
System

by
Yang Zhang

A THESIS

submitted to

Oregon State University

in partial fulfillment of
the requirements for the
degree of

Master of Science

Presented May 10, 2017
Commencement June 2017

Master of Science thesis of <u>Yang Zhang</u> presented on <u>May 10, 2017</u>.

APPROVED:

_____

Major Professor, representing Electrical and Computer Engineering

_____

Director of the School of Electrical Engineering and Computer Science

_____

Dean of the Graduate School

I understand that my thesis will become part of the permanent collection of Oregon State University libraries. My signature below authorizes release of my thesis to any reader upon request.

_____

Yang Zhang, Author

ACKNOWLEDGEMENTS

TABLE OF CONTENTS

LIST OF FIGURE

LIST OF FIGURE (Continued)

LIST OF ALGORITHMS

1 Introduction

In recent years, wireless communication technologies have already been developed and maturely applied to daily using. However, due to the increasing demand for transmission bandwidth, the limitation of Radio Frequency (RF) spectrum is still a critical problem in wireless communication. Lots of research has been published to solve the spectrum limitation issue such as dynamic spectrum access (DSA) approach. However, many of these approaches demand complex RF hardware architecture or relevant algorithms that result in a high power consumption. On the other hand, studies on Free Space Optical (FSO) communication introduce a complementary approach to enhance wireless transmission bandwidth with minimal modification on the existing WiFi system. In FSO research, the solid-state lighting technology is utilized by using Light-Emitting Diodes (LEDs) and Vertical-Cavity Surface-Emitting Lasers (VCSEL) to transmit date at high speed. Additionally, there is no interference between FSO and RF transmissions. However, these FSO applications [1] [2] [3] are limited to spotlight, point to point communication in short distances. And these applications have not been well integrated with the existing WiFi architecture. Thus, WiFO − a hybrid femtocell architecture based on WiFi and Free Space Optical (FSO) technologies is introduced to significantly increase the wireless throughput of existing WiFi networks [4].
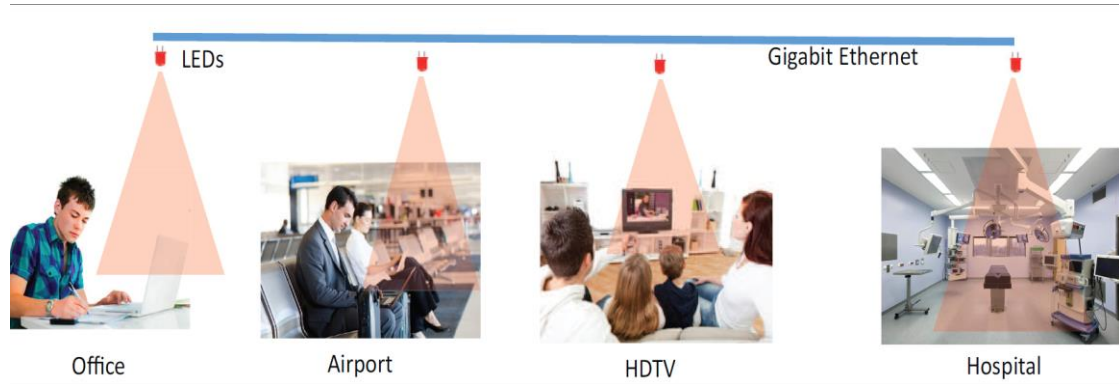
Fig. 1. 1 WiFO use scenarios

1.1 WiFO

WiFO is a hybrid indoor wireless communication system that combines WiFi system and the FSO communication technology. Besides the existing WiFi network, FSO transmitters are developed and deployed under the ceiling following a proper arrangement. The FSO transmitters consist of LEDs and designed circuits that modulate light via Pulse Amplitude Modulation (PAM). Couple potential WiFO application scenarios are shown in Fig. 1.1. To boost up the wireless bandwidth, WiFO can be deployed in offices, airport terminals, entertainment centers and hospitals where cable deployment is costly or unsafe.

To transmit data, each FSO transmitter sheds a light cone directly below in which designed receivers can receive data. In this way, the transmission range of a transmitter can be represented by a circle and the center is the location of that transmitter. A typical example of multiple transmitters' coverage area is shown in Fig. 1.2. Digital signal "1" and "0" are transmitted by switching the LEDs on and off rapidly. Regarding the current system, the switching rate can reach 100 MHz for LED-based transmitters

and greater than 1 GHz for VCSEL based transmitters. According to the general PAM scheme, signals of multiple levels can be transmitted by varying the LED intensities. Fig. 1.3 indicates the light intensity as the function of the position measured from the center of the cone.
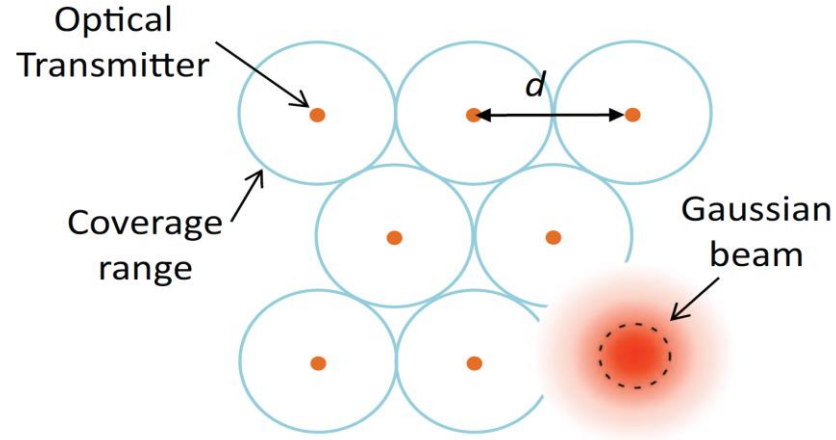
Fig. 1.2 Configuration of the optical transmitter array
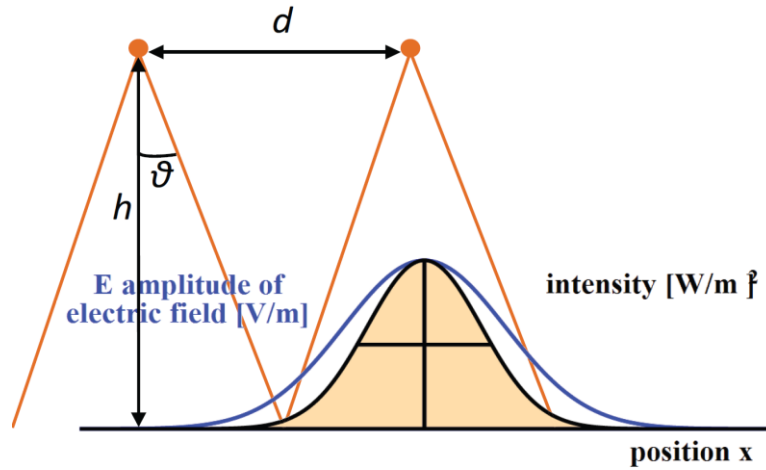
Fig. 1.3 Coverage of optical transmitters with a divergent angle of ϑ

At the receiving side, designed WiFO receiver equipped with a photodiode which converts light intensity into current that can be quantified to stand for digital signal "0" and "1". Based on the position, users with receiving devices can receive data from either FSO channel or WiFi. Access Point (AP) is the brain of the WiFO system that controls the data transmission. The AP decides whether to send data through FSO channel or WiFi. If the data is sent via FSO channel, while receiving, the receiver sends an acknowledgment (ACK) message back to AP via the WiFi channel. Such that, WiFO system can effectively make decisions according to the current network conditions. If the AP decides to send the data via WiFi channel, then the transmission performs like what the usual WiFi network does. Fig. 1.4 shows the detail on how data is transmitted in WiFO system.

While a user with receiving device moves from one light cone to another, the AP automatically detects its location and selects the appropriate transmitter to transmit the data. The transition between WiFi and FSO channel is quickly enough to avoid interruption of packets transmission. Furthermore, even when users are staying outside the light cone, all the data will be automatically sent via the existing WiFi channel.
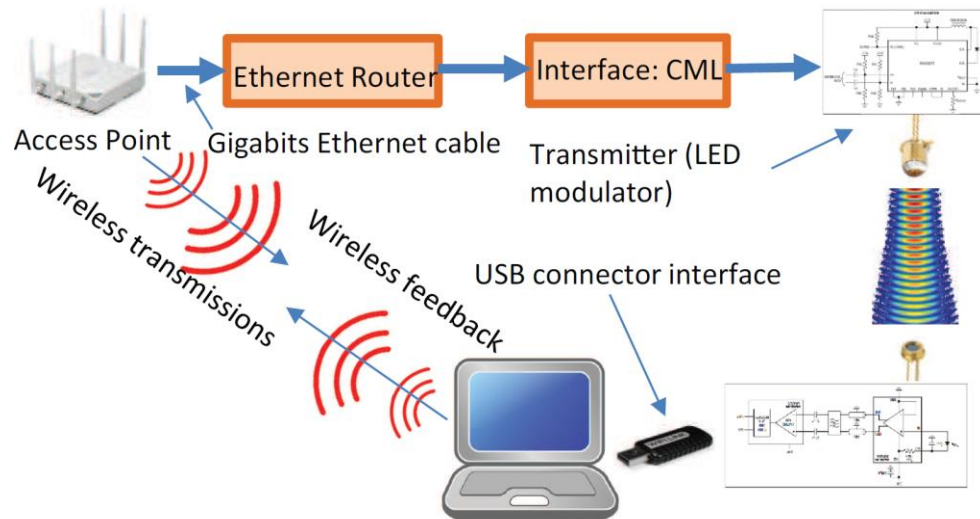
Fig 1.4 Data flow in WiFO

1.2 Contributions: Coverage Algorithms

Coverage problem is a fundamental issue in wireless communication. It is often studied in Wireless Sensor Network (WSN) research. A WSN consists lots of sensor nodes, which are used to perform monitoring, computation and transmission. There are two aspects to be concerned [5], from the viewpoint of sensor device, a particular area should be covered by the sensor. Generally, the sensing ranges of various sensors are considered as unit circles or non-unit circles, and how much covered area or how many covered points are concerned [6]. On the other hand, from the perspective of sensor nodes, in the ad-hoc network among sensor nodes and relay nodes that prolong network lifetime while maintaining connectivity, coverage is concerned by determining whether the nodes are within the transmission range [7].

The coverage problem we discussed is related to transmitter deployment under WiFO system model. In most buildings, Users are highly distributed according to

particular indoor facilities rather than uniformly distributed. Which means some locations require much more transmission power or transmitters than the ones where there are few people. Consequently, to satisfy the user requirement, a proper transmitters' arrangement is essential.

In this thesis, we will focus on coverage algorithms for deployment of WiFO that take advantages of small cell size, line of sight transmissions, and the Gaussian attenuation model of light intensity. Specifically, two types of coverage scenarios - the non-overlapped and the overlapped coverage are presented. For the non-overlapped coverage (packing), we show the bounds of coverage efficiency for a finite rectangle area based on a simple model. For the overlapped coverage, user's SNR profiles are assumed to be given. Using these, three algorithms for determining the optimized deployment based on user's SNR profiles and Gaussian light attenuation models are proposed and evaluated.

2 Related Work

The geometric circle packing problems are often related to facilities deployment problems in wireless networking. Circle packing is to determine how densely a number of disjoint unit circles can be packed together. In [8], Thue, et al. first showed that the regular hexagonal structure is the densest circle packing arrangement with the density of $\pi/\sqrt{12}$. The first rigorous proof was provided by László Fejes Tóth in 1940. In [9], the discrete unit disk cover (DUDC) problem is demonstrated from set covering perspective. A feasibility check whether each point in the set $\mathcal{P}$ of n points could be covered by at least one disk in the set $\mathcal{D}$ of m unit disks, an associated 18-factor approximation algorithm with the running time $O(n \log n + m \log m + mn)$ are proposed. The facility arrangement problems have also been addressed in several papers [10]. Similarly, two different algorithms for efficient sensors' arrangement are first illustrated [11] under the constraints of sufficient grid points coverage. Moreover, in [12], authors made a contribution to Under Water Acoustic Sensor Networks (UW-ASN). Deployment analysis under two-dimensional and three-dimensional architectures are firstly discussed. However, unlike ours, a majority of these works are focused on the coverage without considering the coverage intensity.

3 WiFO System Coverage Problem

We study two types of coverage: Non-overlap coverage or packing and overlapped coverage for WiFO. Specifically, we consider the area to be covered to be a rectangle since this is the most common shape for any room in a building. The goal is to determine the optimal locations of the FSO transmitters.

3.1 Non-overlap Coverage

We analyze the coverage rate for the target rectangular area that is covered by disjoint circles that model the transmission cones of WiFO. In this case, we assume a simple model where if a receiver is in any transmission circle, then it is covered. It is not covered otherwise. The goal is to determine the ratio of covered areas to the total rectangular area. We note that for infinity coverage area, the problem has been solved and the ratio approaches $\pi/\sqrt{12}$. Let r and d be the radius and diameter of the transmission circles where the FSO transmitter is located at the circle center. Let $A = lw$ be the target rectangular area with length l and width w. The coverage rate is η be the area of all the disjoint circles over A. We have the following Proposition.

Proposition 1.

$$\frac{m_l n_l \pi (\frac{d}{2})^2}{wl} \leq \eta \leq 1 - \frac{m_u n_u A_s}{wl} \tag{1}$$

Where:

$$\eta_l = \frac{m_l n_l \pi (\frac{d}{2})^2}{wl} \quad , \quad m_l = \left\lfloor \frac{\frac{w}{d} - 1}{\frac{\sqrt{3}}{2}} + 1 \right\rfloor \quad , \quad n_l = \left\lfloor \frac{l}{d} \right\rfloor$$

$$\eta_u = 1 - \frac{m_u n_u A_s}{wl} \quad , \qquad m_u = \left\lfloor \frac{w}{\frac{\sqrt{3}}{4}d} - 1 \right\rfloor \quad , \qquad n_u = \left\lfloor \frac{l}{d} - \frac{1}{2} \right\rfloor ,$$

$$A_s = \frac{1}{2} \cdot \frac{\sqrt{3}}{2} d^2 - \frac{\pi}{2} \left(\frac{d}{2}\right)^2 = (\frac{\sqrt{3}}{4} - \frac{\pi}{8})d^2 \cong 0.1613 \tag{2}$$

Proof. The proof is based on the densest hexagonal packing that has already been previously established [8]. First, we prove the upper bound. Note that m_u and n_u are the number of the uncovered sections A_s that are completely inside the rectangle in the vertical and horizontal directions, respectively. Similarly, m_l and n_l are the number of circles that are completely inside the rectangle in the vertical and horizontal directions, respectively. In the rectangular area, the uncovered sections A_s always exist and shown in Fig. 3.1. As is the area of the equilateral triangle ABC subtracts the area of half circle, and thus Equation (2) follows.
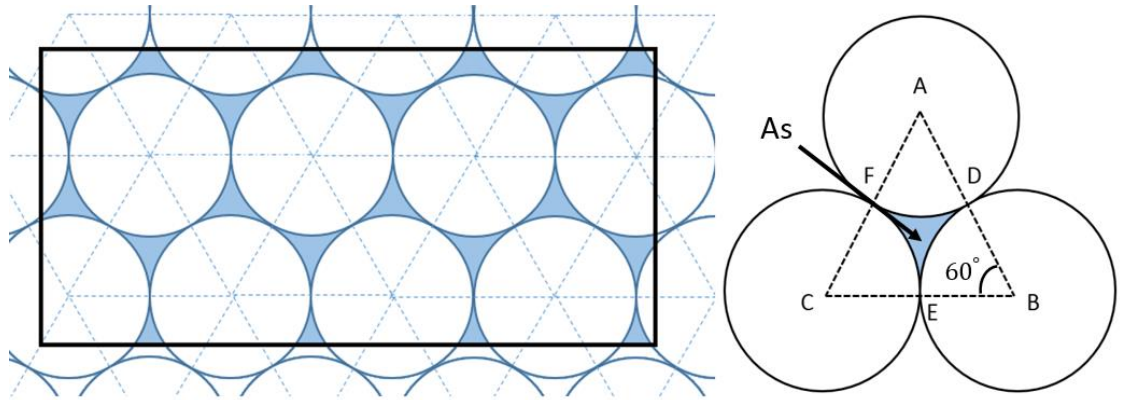

Fig 3.1 Hexagonal Packing and Uncovered Area

Now, to calculate the number of uncovered sections A_S, we introduce a subdivision, by which we divide the target area into small rectangles with length $d/2$ and width $(\sqrt{3}/4)d$. Each small rectangle can completely contain one uncovered section. The subdivision procedure is shown in Fig. 3.2. If there are n_u guaranteed uncovered sections in horizontal direction, then we have

$$(2n_u + 1)\frac{d}{2} \le l < (2n_u + 3)\frac{d}{2} \tag{3}$$

$$\frac{l}{d} - \frac{1}{2} - 1 < n_u \le \frac{l}{d} - \frac{1}{2} \tag{4}$$

$$n_u = \left\lfloor \frac{l}{d} - \frac{1}{2} \right\rfloor \tag{5}$$

Similarly, if there are m_u guaranteed uncovered sections in vertical direction and $m_u \ge 2$, then we obtain

$$(m_u + 1)\frac{\sqrt{3}}{4}d \le w < (m_u + 1 + 1)\frac{\sqrt{3}}{4}d \tag{6}$$

$$\frac{w}{\frac{\sqrt{3}}{4}d} - 2 < m_u \le \frac{w}{\frac{\sqrt{3}}{4}d} - 1 \tag{7}$$

$$m_u = \left\lceil \frac{w}{\frac{\sqrt{3}}{4}d} - 1 \right\rceil \tag{8}$$

Consequently, the guaranteed completely uncovered area is $m_u n_u A_S$. Thus, the upper bound for the coverage rate η_u is

$$\eta_u = 1 - \frac{m_u n_u A_s}{wl}$$

$$\eta_u = 1 - \frac{\left\lceil \frac{w}{\frac{\sqrt{3}}{4}d} - 1 \right\rceil \cdot \left\lceil \frac{l}{d} - \frac{1}{2} \right\rceil \cdot (\frac{\sqrt{3}}{4} - \frac{\pi}{8})d^2}{wl} \tag{9}$$
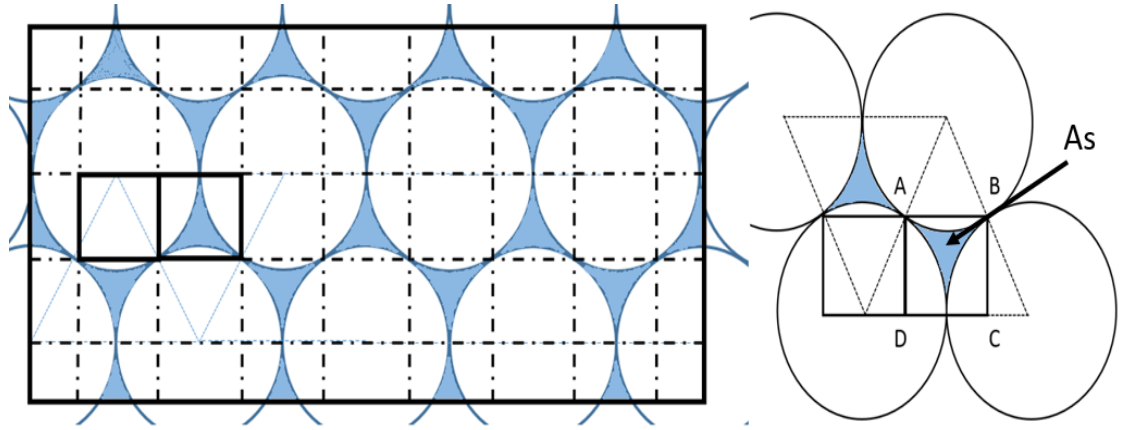

Fig 3.2 Subdivision

The proof of lower bound is similar except that we consider the only circles that are completely inside the rectangle. If there are n_l circles that are completely contained in the horizontal direction, then we have

$$n_l d \leq l < (n_l + 1)d \tag{10}$$

$$\frac{l}{d} - 1 < n_l \leq \frac{l}{d} \tag{11}$$

$$n_l = \left\lfloor \frac{l}{d} \right\rfloor \tag{12}$$

Similarly, if there are m_l completely contained circles in the vertical direction and $m_l \geq 2$, then we obtain

$$\left[(m_l - 1)\frac{\sqrt{3}}{2} + 1 \right] d \leq w < [(m_l + 1 - 1)\frac{\sqrt{3}}{2} + 1]d \tag{13}$$

$$\frac{\frac{w}{d} - 1}{\frac{\sqrt{3}}{2}} < m_l \leq \frac{\frac{w}{d} - 1}{\frac{\sqrt{3}}{2}} + 1 \tag{14}$$

$$m_l = \left\lfloor \frac{\frac{w}{d} - 1}{\frac{\sqrt{3}}{2}} + 1 \right\rfloor \tag{15}$$

Thus, the lower bound for the coverage rate η_l of the target area is,

$$\eta_l = \frac{m_l n_l \pi (\frac{d}{2})^2}{wl}$$

$$\eta_l = \frac{\left\lfloor \frac{\frac{w}{d}-1}{\frac{\sqrt{3}}{2}} + 1 \right\rfloor \cdot \left\lfloor \frac{l}{d} \right\rfloor \cdot \pi (\frac{d}{2})^2}{wl} \tag{16}$$

Therefore, based on equations (1), (2), (9) and (16) the coverage rate η for a given rectangular area with unlimited number of transmitters is,

$$\eta \geq \frac{\left\lfloor \frac{\frac{w}{d}-1}{\frac{\sqrt{3}}{2}} + 1 \right\rfloor \cdot \left\lfloor \frac{l}{d} \right\rfloor \cdot \pi \left(\frac{d}{2}\right)^2}{wl} \tag{17}$$

$$\eta \leq 1 - \frac{\left\lfloor \frac{w}{\frac{\sqrt{3}}{4}d} - 1 \right\rfloor \cdot \left\lfloor \frac{l}{d} - \frac{1}{2} \right\rfloor \cdot (\frac{\sqrt{3}}{4} - \frac{\pi}{8})d^2}{wl} \tag{18}$$

∎

3.2 Overlap Coverage

From the last section, we know it is impossible to cover a rectangular area with disjoint circles. However, 100% covering ratio can be achieved by overlapping the light cones. Consequently, users may receive signals from two or more transmitters if they are standing in the overlapping area. In this section, we consider a specific scenario that

the given rectangular area is completely covered by light cones with the minimum overlapping area. The following figures show three different complete coverage cases. Arbitrary transmitter deployment is shown in Fig. 3.3; hexagonal arrangement with transmitter distance $r < d < \sqrt{3}r$ is shown in Fig. 3.4; hexagonal arrangement with transmitter distance $d = \sqrt{3}r$ is shown in Fig. 3.5.
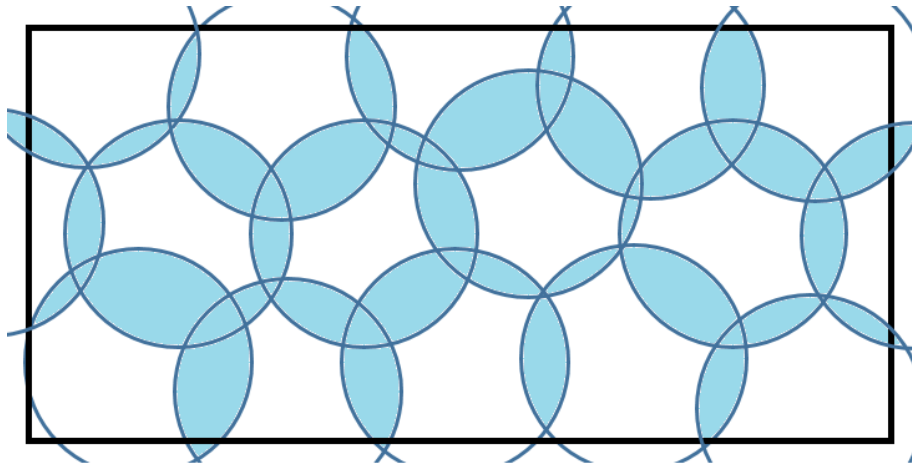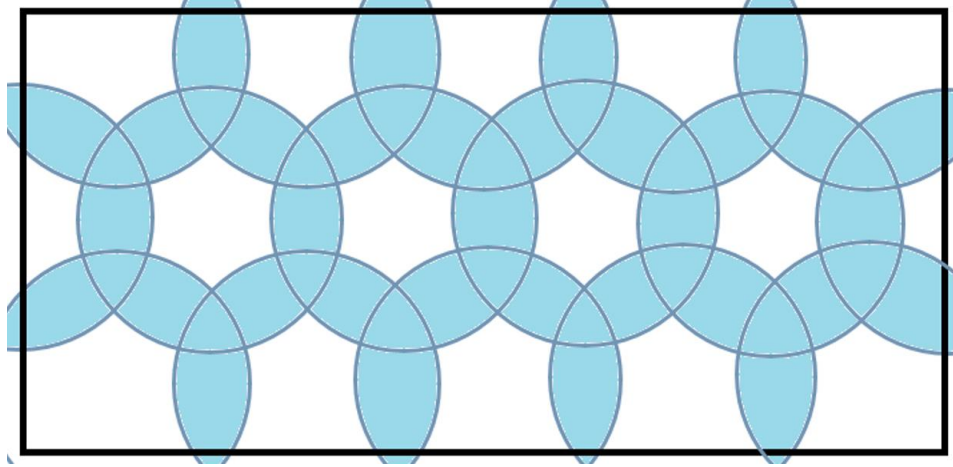

Fig 3.3 Arbitrary Configuration
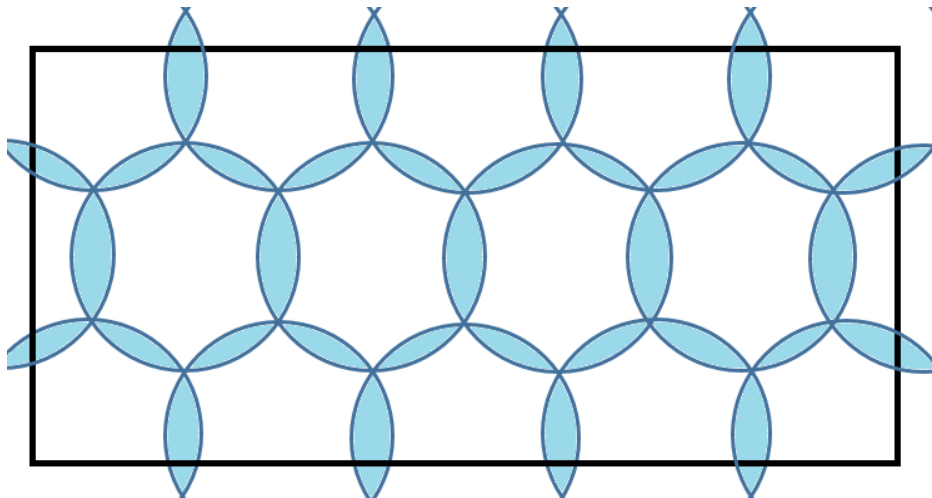
Fig 3.4 Hexagonal Arrangement with $r < d < \sqrt{3}\, r$

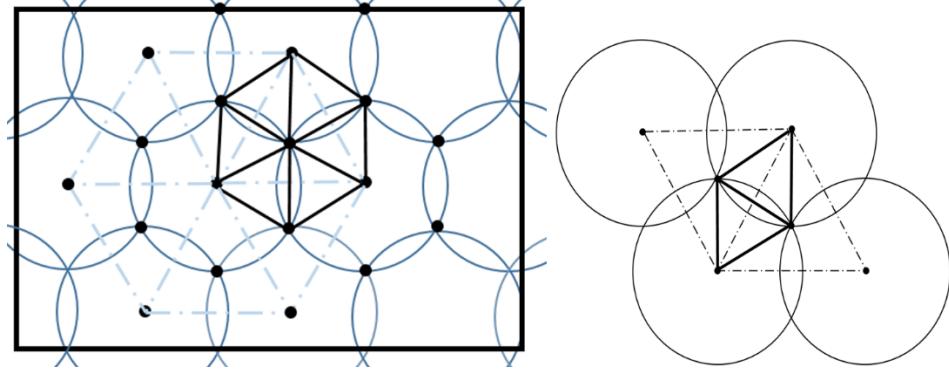Fig 3.5 Hexagonal Arrangement with $d = \sqrt{3}\, r$

Fig 3.6 Delaunay Triangulation for New Configuration

When two or more circles are overlapped, intersection points are generated. Combining the original centers of the circles and the generated intersection points, a new configuration is introduced, which is shown in Fig. 3.6. The dots on the figure are the union of original transmitter centers and generated intersection points from overlapping. The dash-dot triangles stand for the ones in a Delaunay triangulation [8] for the transmitter points, while the solid line triangles represent the ones in a Delaunay triangulation for the new configuration.

Then applying the Delaunay triangulation mechanism [8], the new configuration is also the densest only if it is hexagonal. In other words, all the triangles in the Delaunay triangulation are regular triangles. Therefore, in Fig. 3.7, the points D, E and F will converge on the point O, which is the Fermat point of triangle ABC. Consequently, we have the relation $\frac{d/2}{r} = \sin(\pi/3)$, which is $d = \sqrt{3}r$. Finally, we obtain the condition that $d = \sqrt{3}r$ for completely covering the given area with minimum overlapping area.
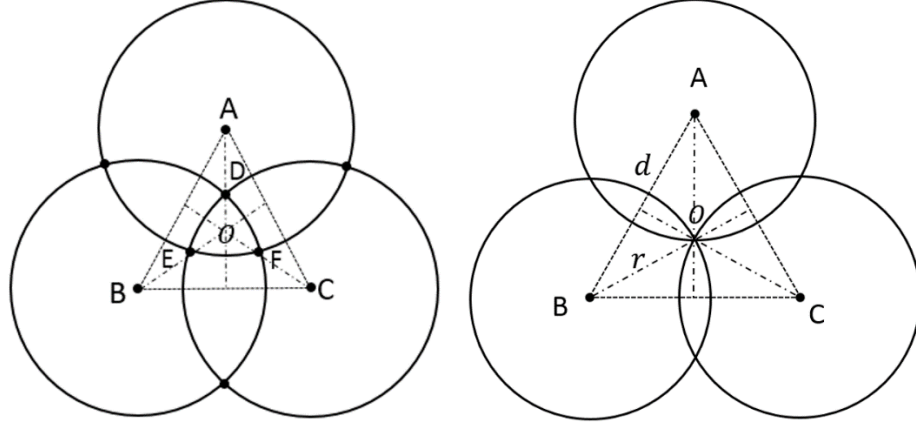
Fig. 3.7 Optimal Structure with η=1

3.3 Users' Signal Matching Pursuit

In contrast to previous sections, we consider the covering problem regarding user's signal intensity within the bounded area. According to the user's distribution, $g(x)$, setting only one transmitter above the area with higher user's density might not be adequate. On the contrary, there is no need to place any transmitters close to the place where few people would like to stay. To meet the requirement that the areas with higher user's density should have priority being covered under the light cones, the difference between user's distribution, $g(x)$ and light intensity distribution, $F(x)$, should be as small as possible, that is,

$$\min \ |g(x) - F(x)| \tag{19}$$

To accomplish (19), we can find out the location of each transmitter in turns by maximizing the convolution of $g(x)$ and $f_i(x)$, which is the ith transmitter's intensity

distribution, i.e. $\max g(x) * f_i(x)$. After current transmitter is found, the user's distribution signal will be updated by subtracting the found transmitter signal. Fig. 3.8 and Fig. 3.9 show the basic concept of obtaining the locations of each $f_i(x)$.
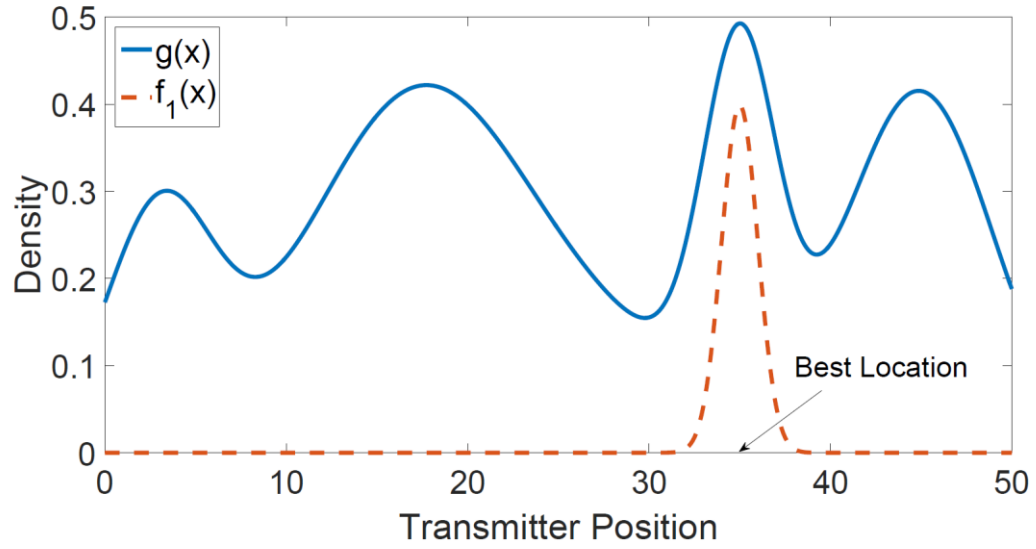

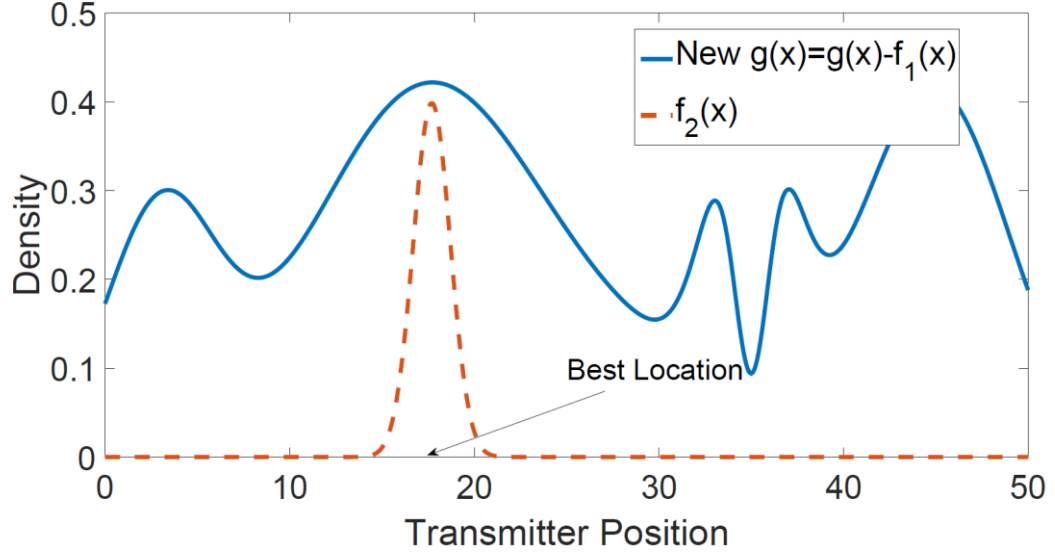Fig. 3.8 Location Detection for 1st Transmitter

Fig. 3.9 Location Detection for 2nd Transmitter

Now, we can extend the case to a 2-dimensional plane, then the light cone signal intensity follows the 2-dimensional normal distribution with uncorrelated independent variables X_1 and X_2. Moreover, two factors (a and σ^2) adjust the intensity and affected area. Our goal is to look for the number and the positions of transmitters with proper parameters to meet the user requirement corresponding to the crowded area.

We introduce and compare three algorithms for transmitter placement according to a given SNR profile. To help us formulate the problem and illustrate the algorithm, we have the following notations defined:

- $f(\mathbf{x}, a, \Sigma)$: Intensity distribution of a transmitter.

  $$f(\mathbf{x}, a, \Sigma) = \frac{a}{\sqrt{(2\pi)^2 |\Sigma|}} e^{-\frac{1}{2}\mathbf{x}^T \Sigma^{-1} \mathbf{x}}$$

- $g(x)$: SNR profile in a given plan.

- $f_i(\mathbf{x})$: Intensity function of the ith transmitter.

$$f_i(\mathbf{x}) = \frac{a_i}{\sqrt{(2\pi)^2|\Sigma_i|}} e^{-\frac{1}{2}(\mathbf{x}-\mu_i)^T \Sigma_i^{-1}(\mathbf{x}-\mu_i)}$$

- $F(\mathbf{x})$: Deployment function of all the transmitters.

$$F(\mathbf{x}) = \sum_i f_i(\mathbf{x})$$

- $\mathbf{x}$: Location coordinates of a 2-dimensional plane.

$$\mathbf{x} = (x_1, x_2)^T$$

- a_i : The light intensity of the ith transmitter.

- μ_i : Location coordinates of the ith transmitter.

$$\boldsymbol{\mu_i} = (\mu_1, \mu_2)^T$$

- $\boldsymbol{\Sigma_i}$: A 2×2 covariance matrix representing the coverage of the ith transmitter.

$$\Sigma_i = \begin{bmatrix} \sigma_i^2 & 0 \\ 0 & \sigma_i^2 \end{bmatrix}$$

- N : The number of transmitters.

The range of parameter $\boldsymbol{\mu}$ is bounded within the target area. The other two factors σ and a are positive real number and limited by the character of transmitter.

3.3.1 Algorithm One

To accomplish the coverage task, we place transmitters into the area one by one. Due to the four factors for a transmitting signal, which are center coordinate $\boldsymbol{\mu}$ including two directions, signal intensity a and signal divergent $\boldsymbol{\Sigma}$, we exam all the factor combinations and choose the best one. Then update the user's signal by

subtracting the current transmitting signal. The next transmitter selection is always based on the updated user's signal. Before introducing one transmitter into the area, a non-zero check is added to block some factor combinations. This procedure is checking whether any points of the adding transmitter is greater than those of the current user's signal. This is to avoid the uncertainty of the negative data introduced during the subtraction. Generally, we want to minimize the value $g(\mathbf{x}) - f(\mathbf{x}, a, \Sigma)$ subject to $f_i(\mathbf{x}) \leq g(\mathbf{x})$. The whole procedure is summarized as:

Algorithm 1 Matching Algorithm with Zero-Check

1: **for** each transmitter $i = 1 : N$ **do**

2:
$$\underset{\mathbf{x}', a, \Sigma}{\text{Max}} \quad g(\mathbf{x}') * f(\mathbf{x}', \mathbf{a}, \Sigma)$$
$$\text{s.t.} \quad min(g(\mathbf{x}) - f(\mathbf{x} - \mathbf{x}', \mathbf{a}, \Sigma)) \geq \mathbf{0}$$

3:      set $\boldsymbol{\mu}_i = \mathbf{x}'^*$, $a_i = a^*$ and $\Sigma_i = \Sigma^*$;

4:      $g(\mathbf{x}) = g(\mathbf{x}) - f_i(\mathbf{x})$;

5: **end for**

6: $F(\mathbf{x}) = \sum_i f_i(\mathbf{x})$;

Algorithm 1   Matching Algorithm with Zero-Check

3.3.2 Algorithm Two

In contrast to Algorithm 1, we ignore the non-zero check, i.e., during each transmitter searching step, we select the best transmitter's signal that matches the current user's signal from all the possible factor combinations. Then update the user's signal by subtracting the selected best transmitting signal. Next, we keep searching best parameters for the next transmitter based on the update. This algorithm minimizes the value $\max(g(\mathbf{x}) - f(\mathbf{x}, a, \Sigma), 0)$ subject to the specific range of the parameters (μ, a and σ^2).

Algorithm 2 Matching Algorithm without Zero-Check

1: **for** each transmitter $i = 1 : N$ **do**

2:
$$\underset{\mathbf{x}', a, \Sigma}{\text{Max}} \quad g(\mathbf{x}') * f(\mathbf{x}', \mathbf{a}, \Sigma)$$
$$\text{s.t.} \quad min|g(\mathbf{x}) - f(\mathbf{x} - \mathbf{x}', \mathbf{a}, \Sigma)|$$

3:      set $\mu_i = \mathbf{x}'^*$, $a_i = a^*$ and $\Sigma_i = \Sigma^*$;

4:      $g(\mathbf{x}) = g(\mathbf{x}) - f_i(\mathbf{x})$;

5: **end for**

6: $F(\mathbf{x}) = \sum_i f_i(\mathbf{x})$;

Algorithm 2. Matching Algorithm without Zero-Check

3.3.3 Algorithm Three

Algorithms 2 and 3 are similar. The only difference is a set-zero procedure is introduced during the user's signal updating. The set-zero procedure goes right after the subtraction that set all the negative date to zero. The rest of the whole algorithm is the same as Algorithm 2.

Algorithm 3 Matching Algorithm with Set-Zero procedure

1: **for** each transmitter $i = 1 : N$ **do**

2:
$$\underset{\mathbf{x}',a,\mathbf{\Sigma}}{\text{Max}} \quad g(\mathbf{x}') * f(\mathbf{x}', \mathbf{a}, \mathbf{\Sigma})$$
$$\text{s.t.} \quad min|g(\mathbf{x}) - f(\mathbf{x} - \mathbf{x}', \mathbf{a}, \mathbf{\Sigma})|$$

3:      set $\boldsymbol{\mu}_i = \mathbf{x}'^*$, $a_i = a^*$ and $\Sigma_i = \Sigma^*$;

4:      $g(\mathbf{x}) = g(\mathbf{x}) - f_i(\mathbf{x})$;

5:      **for v in x do**

6:          **if** $g(\mathbf{v}) < 0$ **then**

7:             **Set** $g(\mathbf{v}) = 0$;

8:          **end if**

9:      **end for**

10: **end for**

11: $F(\mathbf{x}) = \sum_i f_i(\mathbf{x})$;

Algorithm 3 Matching Algorithm with Set-Zero Procedure

4 Simulation Result

We show simulation results to verify and compare the proposed algorithms. We apply three algorithms on the same model that is in a finite 15×15 area, an arbitrary SNR profile. With regard to the signal for a transmitter, the intensity factor a and divergent factor σ are both chosen from 0.5 to 4 to represent the shape of light cones which can be controlled. We run the algorithms for scenario consisting of 1 to 11 transmitters. Fig. 4.1 shows the contour of the original SNR profile. For the transmitter number $N = 3$, Fig. 4.2, Fig. 4.4 and Fig. 4.6 show the SNR profiles and transmitters' deployment after running three algorithms 1, 2, and 3, respectively. The contours of remaining SNR profiles are shown in Fig. 4.3, Fig. 4.5 and Fig. 4.7 respectively.

For the transmitter number $N = 6$, Fig. 4.8, Fig. 4.10 and Fig. 4.12 show the SNR profiles and transmitters' deployment after running three algorithms 1, 2, and 3, respectively. The contours of remaining SNR profiles are shown in Fig. 4.9, Fig. 4.11 and Fig. 4.13 respectively. We note that since the remaining SNR profiles are the difference between the target SNR and what WiFO can provide, the smaller values of the remaining SNR profiles, the better are the algorithms. As observed, the Algorithm2 and Algorithm3 are quite close, and both are better than Algorithm1. Fig. 4.14 shows the comparison of the accumulative remaining SNR for three algorithms applied using the number of transmitters from 1 to 11. With the number of transmitters increasing, the Algorithm 3 outperforms the others with the smallest resulted error.
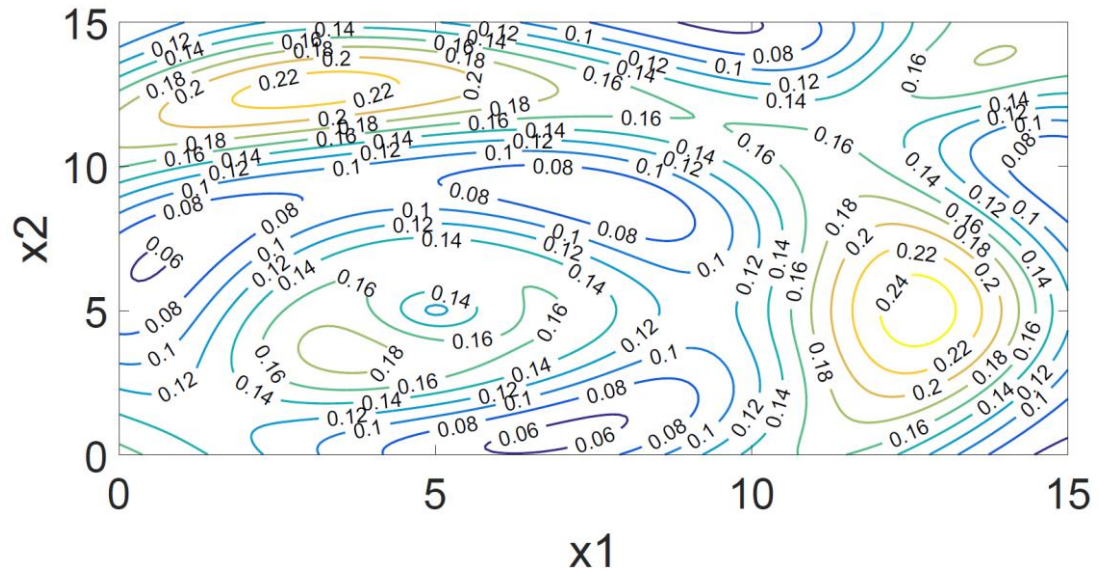
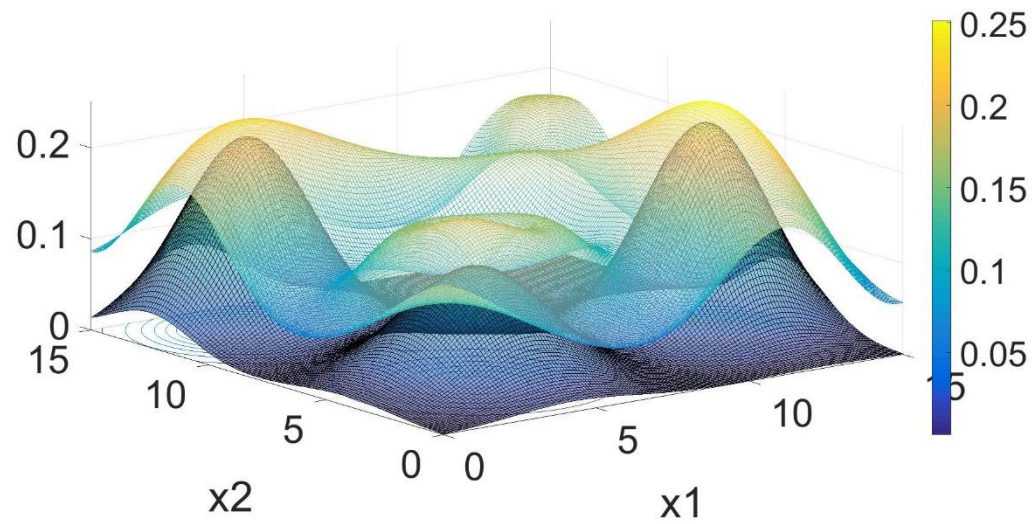Fig. 4.1 Contour of a given SNR profile

Fig. 4.2 SNR profile and Transmitters Deployment after running Algorithm 1 (N=3)

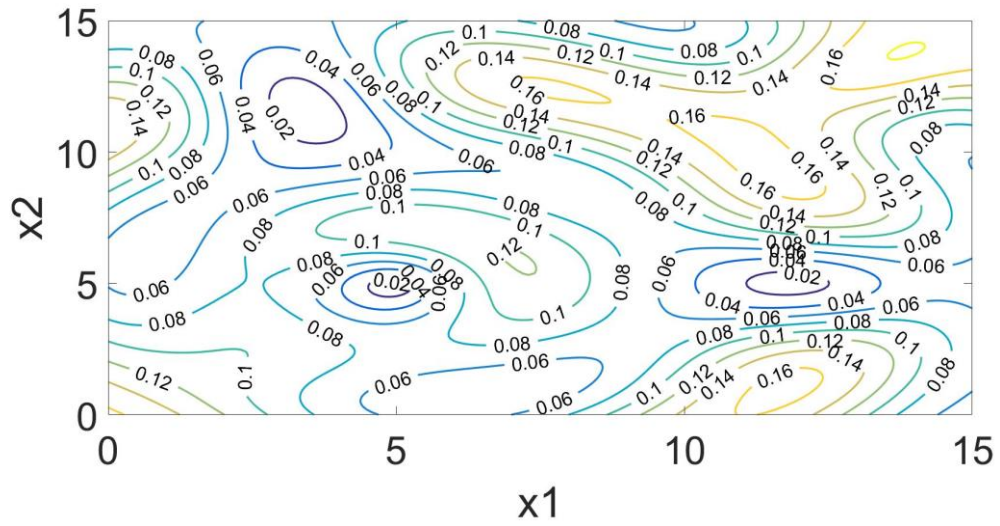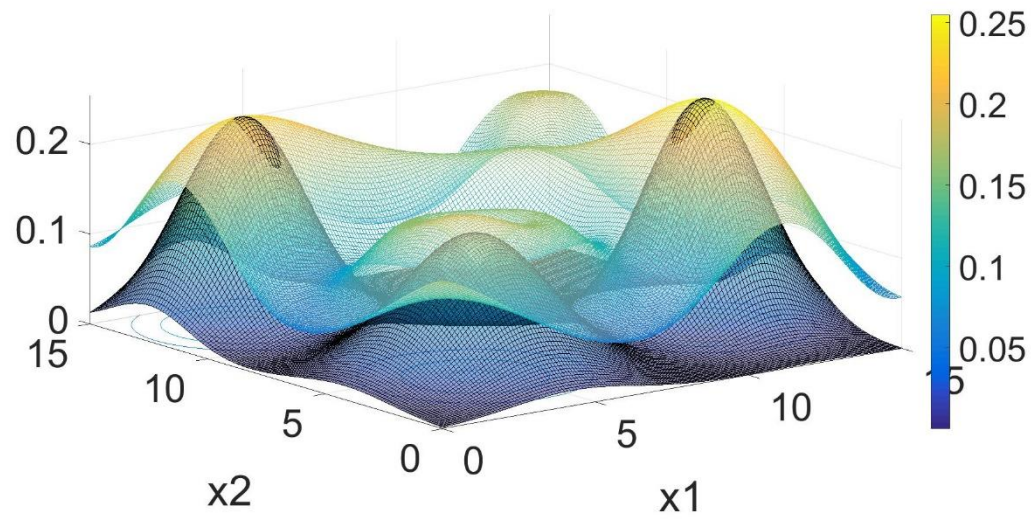Fig. 4.3 Contour of remaining SNR profile after running Algorithm 1 (N=3)

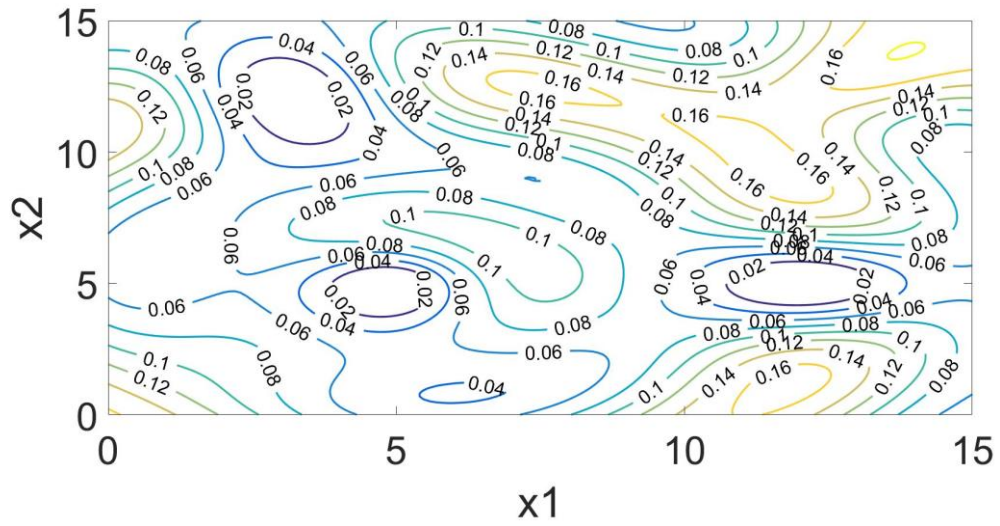Fig. 4.4 SNR profile and Transmitters Deployment after running Algorithm 2 (N=3)

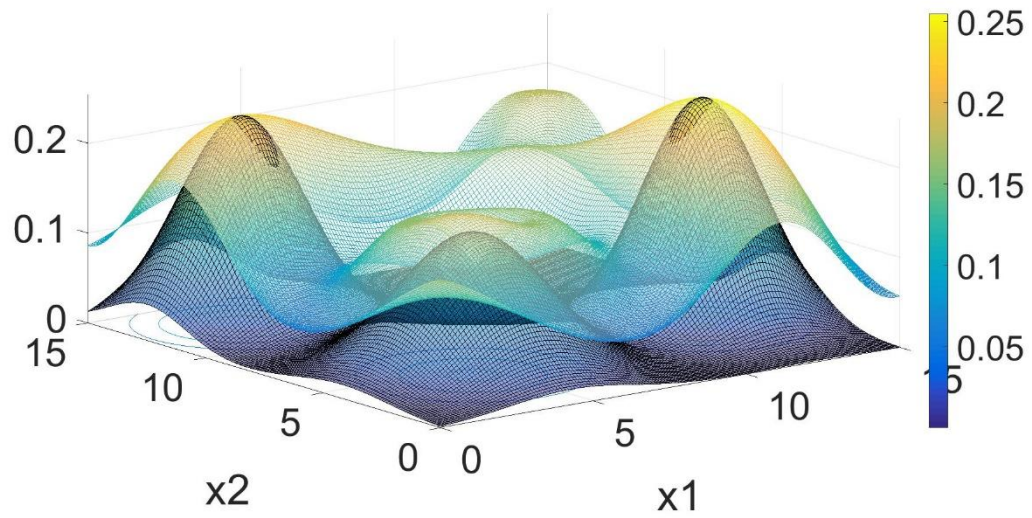Fig. 4.5 Contour of remaining SNR profile after running Algorithm 2 (N=3)

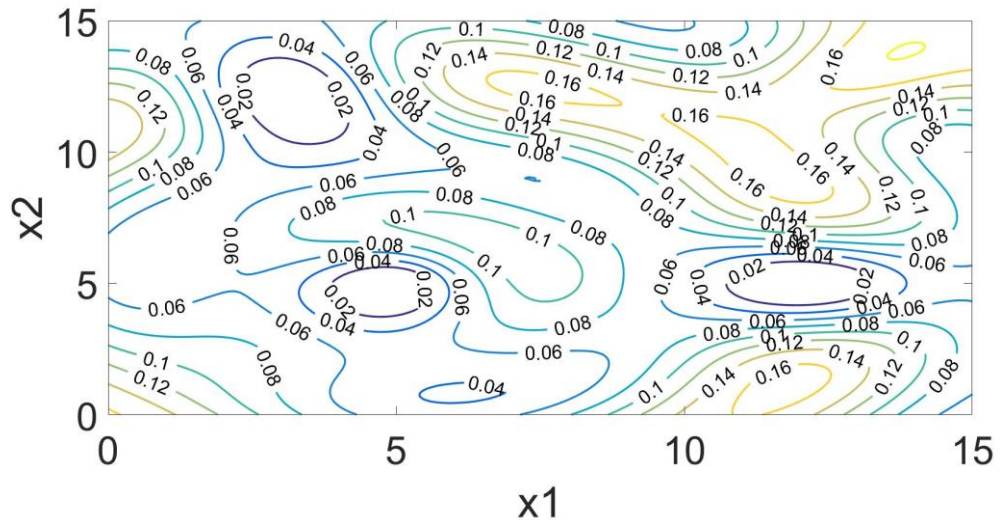Fig. 4.6 SNR profile and Transmitters Deployment after running Algorithm 3 (N=3)

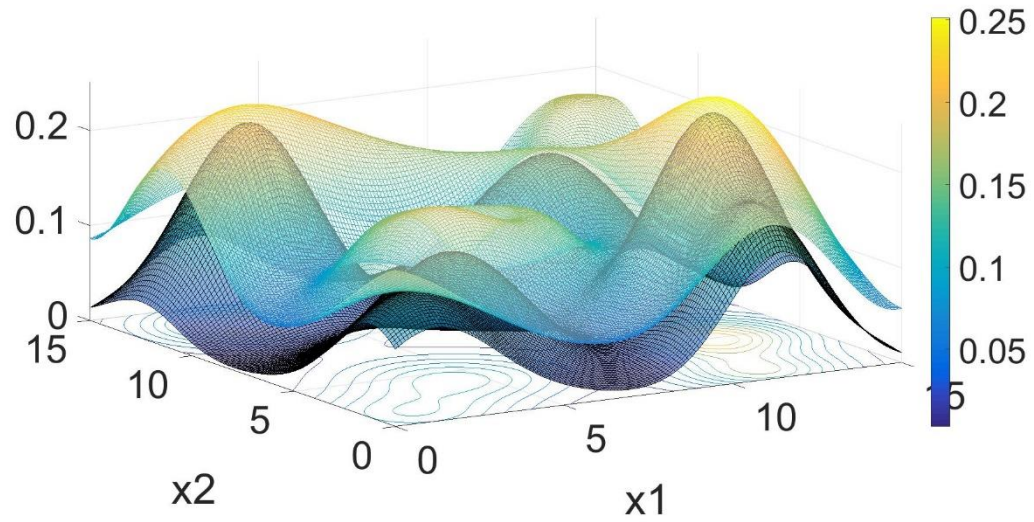Fig. 4.7 Contour of remaining SNR profile after running Algorithm 3 (N=3)

2

Fig. 4.8 SNR profile and Transmitters Deployment after running Algorithm 1 (N=6)
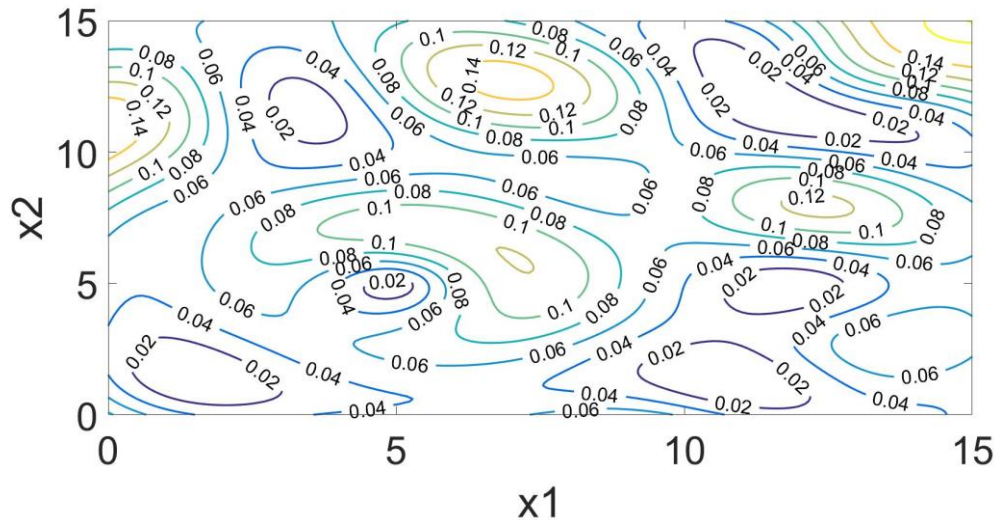
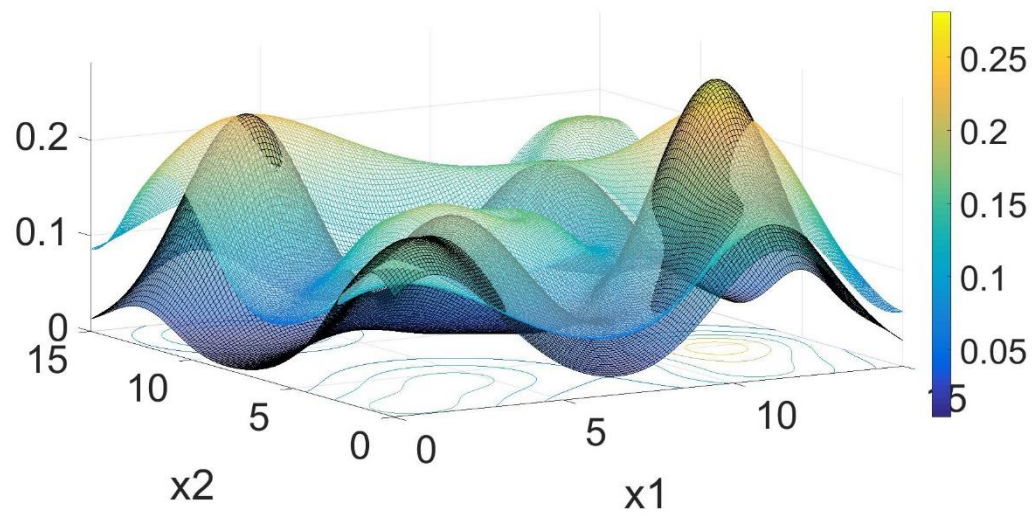Fig. 4.9 Contour of remaining SNR profile after running Algorithm 1 (N=6)

Fig 4.10 SNR profile and Transmitters Deployment after running Algorithm 2 (N=6)
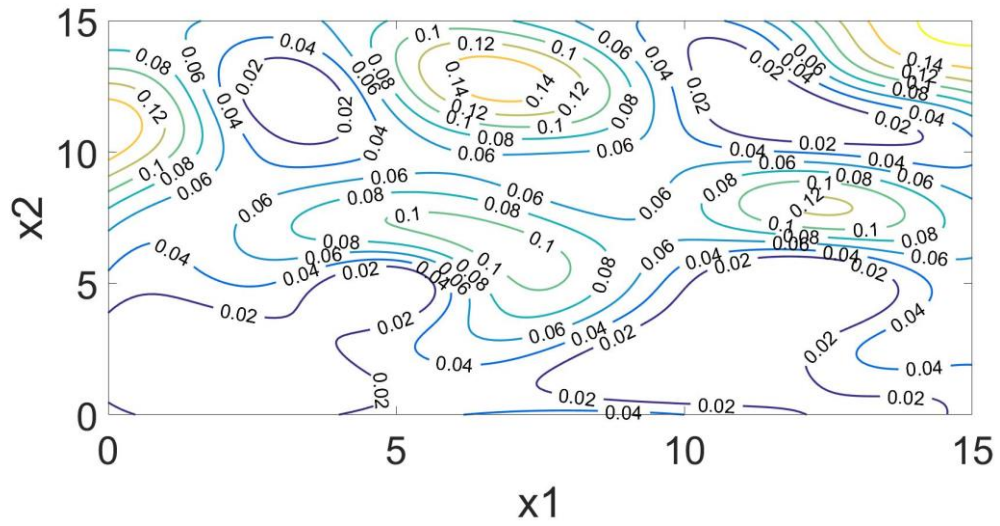
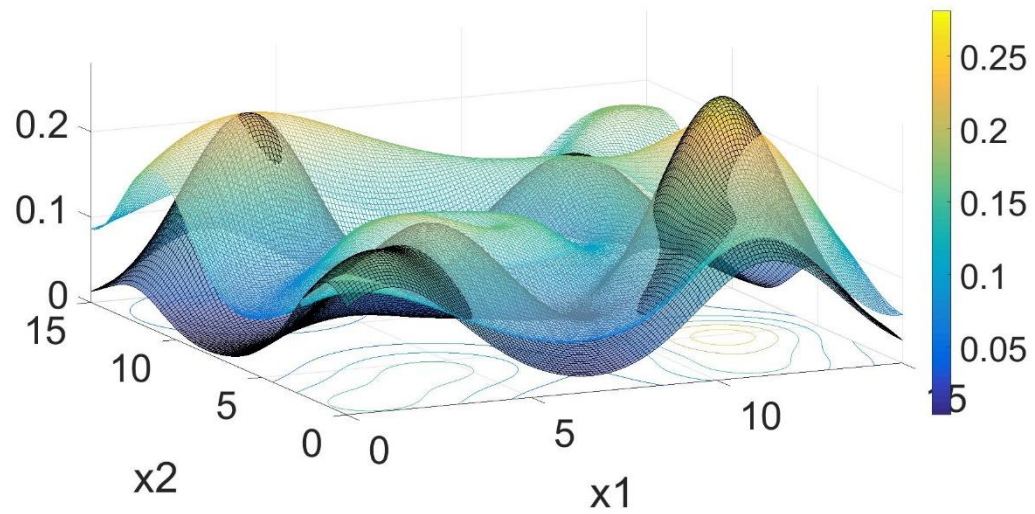Fig. 4.11 Contour of remaining SNR profile after running Algorithm 2 (N=6)

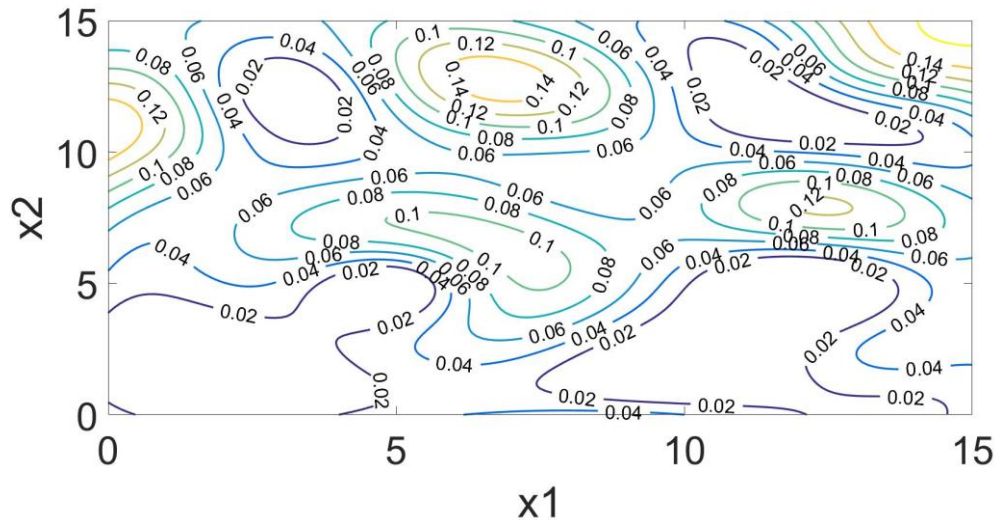Fig 4.12 SNR profile and Transmitters Deployment after running Algorithm 3 (N=6)

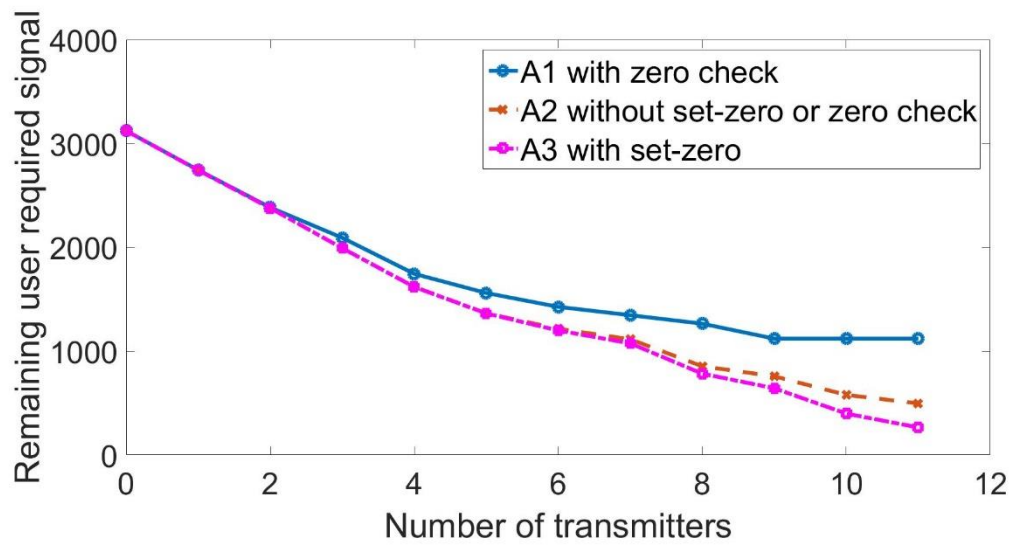Fig. 4.13 Contour of remaining SNR profile after running Algorithm 3 (N=6)

Fig. 4.14 Comparison of overall remaining errors for 3 Algorithms

5 Conclusion

In this paper, we introduce the densest circle packing within a finite area and a bounded covering rate is provided with numerical analysis. Additionally, the condition for complete coverage scenario is discussed. Finally, three matching pursuits for transmitter deployment according to the distribution of users are proposed. From the simulation result, the algorithm with set-zero procedure during each step is the best one.

Bibliography

[1] H. Wu, B. Hamzeh and M. Kavehrad, Achieving carrier class availability of fso link via a complementary rf link, Signals, Systems and Compputers, 2004. Conference Record of the Thirty-Eighth Asilomar Conference, vol. 2, pp. 1483-1487, Nov. 2004.

[2] S. Bloom and W. Hartley, The last-mile solution: hybrid FSO radio, AirFibber Inc., May. 2002.

[3] I. Kim and E. Korevaar, Availability of free space optics (fso) and hybrid fso/rf systems, Proc. Optical Wireless Commun. IV, Aug. 2001.

[4] Q. Wang, T. Nguyen, and A. X. Wang, Channel Capacity Optimization for an Integrated Wi-Fi and Free-Space Optic Communication System (wififo), In Proceedings of the 17th ACM international conference on Modeling, analysis and simulation of wireless and mobile system, pages 327-330. ACM, 2014.

[5] K. Kar and S. Banerjee, Node Placement for Connected Coverage in Sensor Networks, WiOp'03: Modeling and Optimization in Mobile, Ad Hoc and Wireless Networks, France, Mar 2003.

[6] C. Huang and Y. Tseng, The Coverage Problem in a Wireless Sensor Network, Mobile Networks and Applications, 10(4)519528, 2005.

[7] E. L. Lloyd and G. Xue, Relay Node Placement in Wireless Sensor Networks, IEEE Transactions on Computers, 56(1):134-138, 2007.

[8] H. Chang and L. Wang, A Simple Proof of Thue's Theorem on Circle Packing, arXiv:1009.4322v1 [math.MG], 2000.

[9] G. K. Das, R. Fraser, A. Lopez-Ortiz, and B. G. Nickerson, On The Discrete Unit Disk Cover Problem, International Journal of Computational Geometry & Applications, 22(5):407419, 2012.

[10] J. J. Gonzalez-Barbosa, T. Garcia-Ramirez, J. Salas, J. B. Hurtado- Ramos, and J. D. J. Rico-Jimenez, Optimal camera placement for total coverage, IEEE International Conference on Robotics and Automation, 2009.

[11] S. Dhillon and K. Chakrabarty, Sensor placement for effective coverage and surveillance in distributed sensor networks, IEEE Wireless Communications and Networking, 2003.

[12] D. Pompili, T. Melodia, and I. F. Akyildiz, Deployment analysis in underwater acoustic wireless sensor networks, Proceedings of the 1st ACM international workshop on Underwater networks - WUWNet '06, 2006.